Chemical Displacement of Molecules Adsorbed on Copper Surfaces: Low-Temperature Studies with Applications to Surface Reactions

P. W. Kash,[†] M. X. Yang,[‡] A. V. Teplyakov, G. W. Flynn,* and B. E. Bent[§]

Department of Chemistry, Columbia University, New York, New York 10027

Received: February 13, 1997; In Final Form: July 7, 1997[⊗]

Previous experiments have demonstrated that displacement of a molecule adsorbed on a metal surface by an impinging gas-phase molecule can be quite a facile process. The generality of this process for an enthalpic driving force as small as 1 kcal/mol is demonstrated here using the displacement of a weakly binding alkene, cyclopentene, by a series of more strongly binding alkenes on Cu(100). Surface structure sensitivity in the process is also demonstrated by a comparison of benzene and cyclopentene coadsorption on Cu(100) and Cu(110). This work also shows the utility of conducting the displacement process below the temperature at which the displaced molecule desorbs from the multilayer so that temperature-programmed desorption can be used to quantify the surface coverage of displaced molecules. It is also shown that one can readily determine the kinetics of adsorbate bond dissociation and bond formation reactions by combining these chemical displacement measurements of surface coverage with an anneal/quench protocol. This approach is demonstrated through chemical displacement experiments that determine that the C−Br bond in vinyl bromide adsorbed on Cu(100) dissociates near 157 K and that the formation of toluene from reaction between methyl iodide and coadsorbed phenyl groups on Cu(110) occurs below 160 K. The relative importance of enthalpy and entropy in chemical displacement is also discussed.

I. Introduction

An important phenomenon in the interaction of adsorbed monolayers with bulk phases is the replacement of surface-adsorbed molecules by molecules from the bulk phase. This type of monolayer replacement plays a key role in processes such as heterogeneous catalysis where replacement of surface-generated products by bulk phase reactants is required for catalytic turnover. Interestingly, while monolayer replacement can occur simply by desorption from the monolayer followed by adsorption from the bulk, there are now numerous examples where it is clear that replacement is a concerted process in which molecules from the bulk phase assist the desorption of adsorbates from the monolayer. Examples include displacement chromatography,[1] surface exchange of adsorbed polymers in thin films,[2−6] solute/solvent exchange at the liquid/solid interface,[7a,b] acid−base displacement,[8a,b] competitive adsorption of proteins at biologically relevant interfaces,[9] and surfactant-mediated growth of metal[10−12] and semiconductor[13] thin films.

In each of these examples, monolayer replacement occurs at a rate that is orders of magnitude faster than the rate of desorption from the monolayer in the absence of the bulk phase. It is thus appropriate to view these replacement events as displacement processes in which adsorbed species are displaced from the monolayer by molecules from the bulk phase. To distinguish these displacement processes from the removal of monolayers by physical sputtering, we use the term "chemical displacement". For simple adsorbates and single monolayers, chemical displacement is the surface analogue of ligand displacement in inorganic and organometallic chemistry.[14] In fact, the understanding gained from studies of the chemical displacement of monolayers at the vacuum/solid interface where the solvent effects can be precisely controlled may provide important insights into ligand exchange in molecular complexes.

The focus of the current work is the demonstration and application of chemical displacement for the study of adsorbed monolayers and reactions at the vacuum/solid interface. Previous studies that are directly relevant to the current work are summarized in Tables 1−3. All of these studies involve the chemical displacement of monolayers at the vacuum/solid interface at temperatures significantly below where the adsorbed species would thermally desorb in the absence of the displacing agent. In some cases, the displacing agent is simply an isotope of the adsorbed molecule[15−20] and the exchange process observed demonstrates the facility with which monolayers equilibrate with gas-phase species. More commonly, the displacing agent is chemically different from the adsorbed species and there is an enthalpic driving force[15−17,22−36] for this adsorption-assisted desorption (see Table 1). In other studies, it appears that part of the effectiveness of the displacing agent (e.g., H_2) may be due to the fact that it dissociates upon adsorption.[37−42] Results of these dissociation-induced chemical displacement studies are summarized in Table 2. Although there is some uncertainty as to whether it is the displacement that permits dissociation or the dissociation that drives displacement, a number of recent results, also summarized in Table 2, provide convincing evidence that dissociation of adsorbed species can drive the displacement of molecules that are coadsorbed in the monolayer.[43,44] All of the studies in Tables 1 and 2 have been carried out at temperatures above where the displaced species desorbs from the second layer. A number of studies, however, have demonstrated that chemical displacement can be sufficiently facile that low-temperature displacement from the monolayer to a stable multilayer is possible.[18−20,28,45−51] These results, which are summarized in Table 3, are particularly relevant to the studies reported here where temperature-programmed desorption (TPD) of molecules displaced to the second layer will be used to quantify the extent of reaction in

[†] NSF Postdoctoral Fellow. Present address: Department of Chemistry, University of British Columbia, Vancouver, B.C., Canada.
[‡] Present Address: Materials Science Division, Building 66, Lawrence Berkeley National Laboratory, Berkeley, CA 94720.
[§] Camille and Henry Dreyfus Teacher Scholar; deceased.
* To whom correspondence should be addressed. Telephone: (212) 854-4162. Fax (212) 932-1289. E-mail: flynn@chem.columbia.edu.
[⊗] Abstract published in *Advance ACS Abstracts,* September 1, 1997.

S1089-5647(97)00563-4 CCC: $14.00

TABLE 1: Adsorption Assisted Desorption

system	comment	ref
$Ni(100)/C^{18}O + C^{16}O \rightarrow Ni(100)/C^{16}O + C^{18}O$	$T_{surface} < 200$ K	D. W. Goodman et al.[15] (1980)
$Pd/C^{18}O + C^{16}O \rightarrow Pd/C^{16}O + C^{18}O$	$T_{surface} = 339-466$ K	T. Yamada et al.[16] (1983)
$W(100)/C_2D_6 + C_2H_6 \rightarrow W(100)/C_2H_6 + C_2D_6$	$T_{surface} = 110$ K	A. C. Liu et al.[17] (1989)
$Ir(110)/H + CO \rightarrow Ir(110)/CO + H_2$	$T_{surface} = 130$ K	D. E. Ibbotson et al.[21] (1980)
$Ni(100)/C_6H_6 + P(CH_3)_3 \rightarrow Ni(100)/P(CH_3)_3 + C_6H_6$	Benzene detected as intermediate in hydrocarbon decomposition reaction. Also on Ni(111), Ni[9(111) × (111)], and Ni[7(111) × (111)]	M. C. Tsai et al.[22] (1982) M. C. Tsai et al.23 (1982) C. M. Friend et al.[24] (1981)
$Pt(100)/C_6H_6 + P(CH_3)_3 \rightarrow Pt(100)/P(CH_3)_3 + C_6H_6$	Benzene detected as intermediate in hydrocarbon decomposition. Also on Pt(111) and Pt[6(111) × (111)]	M. C. Tsai et al.[25] (1982) M. C. Tsai et al.[23] (1982) M. C. Tsai et al.[26] (1982)
$Pt(111)/CO + PH_3 \rightarrow Pt(111)/PH_3 + CO$	$T_{surface} = 100$ K	G. E. Mitchell et al.[27] (1987)
$Pt(111)/C_6H_{10} + Bi \rightarrow Pt(111)/Bi + C_6H_{10}$	bismuth postdosing thermal desorption mass spectroscopy	C. T. Campbell et al.[28] (1988) F. C. Fenn et al.[29] (1989)
$Ni(100)/CO + NO \rightarrow Ni(100)/NO + CO$	$T_{surface} = 140$ K $T_{surface} = 160$ K, oriented NO beam $T_{surface} = 300$ K, oriented NO beam $T_{surface} = 310$ K	A. V. Hamza et al.[30] (1998) H. Muller et al.[31] (1992) H. Muller et al.[32] (1994) M. Kawai et al.[33] (1994)
$Al_2O_3/Rh/CO + PH_3 \rightarrow Al_2O_3/Rh/PH_3 + CO$	$T_{surface} = 90$ K	G. Lu et al.[34] (1990)
$Pt(111)/O_2 + CO \rightarrow Pt(111)/CO + O_2$	$T_{surface} = 100$ K, CO beam	C. Akerlund et al.[35] (1994)
$Pt(111)/O_2 + H, N, O \rightarrow Pt(111)/H, N, O + O_2$	$T_{surface} = 80$ K	J. Lee et al.[36] (1994)

TABLE 2: Dissociation-Induced Desorption

system	comment	ref
$W(100)/H + D_2 \rightarrow W(100)/D + H_2$	$T_{surface} = 298$ K	L. D. Schmidt et al.[37] (1970)
$Ni(100)/CO + H_2 \rightarrow Ni(100)/H + CO$	$T_{surface} = 309-330$ K	C. S. Shen et al.[38] (1988) J. L. Gland et al.[39] (1990)
$Pt(111)/CO + H_2 \rightarrow Pt(111)/H + CO$	$T_{surface} = 309-328$ K $T_{surface} = 130-400$ K $T_{surface} = 318-348$ K	J. L. Gland et al.[39] (1990) D. H. Parker et al.[40] (1990) D. H. Parker et al.[41] (1991)
$Ag(110)/2\ O_2 \rightarrow Ag(110)/2O + O_2$	$T_{surface} = 170$ K	J. T. Roberts et al.[43] (1992)
$Ni(111)/CO + H_2 \rightarrow Ni(111)/H + CO$	See shift in CO desorption temp	R. Zhang et al.[42] (1993)
$Fe(100)/2\ CO \rightarrow Fe(100)/O + Fe(100)/C + CO$	$T_{surface} = 440$ K	M. H. Nassir et al.[44] (1994)

TABLE 3: Chemical Displacement to a Second Layer

system	comment	ref
$Ru(001)/C_6D_6/C_6H_6 + C_6D_6 \rightarrow Ru(001)/C_6D_6/C_6D_6/C_6H_6$	$T_{surface} = 115$ K	P. Jacob et al.[18] (1989) D. Menzel et al.[19] (1989)
$Cu(111)/C_6D_6 + C_6H_6 \rightarrow Cu(111)/C_6H_6/C_6D_6$	$T_{surface} = 110$ K	Xi et al.[20] (1994)
$graphite(0001)/Xe + Kr \rightarrow graphite(0001)/Kr/Xe$	$T_{surface} = 84.5$ K	J. Regnier et al.[45] (1981)
$graphite(0001)/C_6H_{12} + Kr \rightarrow graphite(0001)/Kr/C_6H_{12}$	$T_{surface} = 77$ K	A. Razafitianamaharavo et al.[46] (1990)
$graphite(0001)/CCl_4 + Kr \rightarrow graphite(0001)/Kr/CCl_4$	$T_{surface} = 79$ K	M. Abdelmoula et al.[47] (1992)
$Pt(111)/C_6H_6 + Bi \rightarrow Pt(111)/Bi/C_6H_6$	Benzene detected as intermediate in hydrocarbon decomposition reaction. $T_{surface} = 110$ K	C. T. Campbell et al.[28] (1988) J. A. Rodriguez et al.[48] (1989) J. A. Rodriguez et al.[49] (1989)
$Pt(111)/C_6H_5CH_3 + Bi \rightarrow Pt(111)/Bi/C_6H_5CH_3$	$T_{surface} = 100$ K	M. E. Domagala et al.[50] (1994)
$Pt(111)/H_2O + HCOOH \rightarrow Pt(111)/HCOOH/H_2O$	$T_{surface} = 100$ K	M. R. Columbia et al.[51] (1990)

the monolayer. Particularly noteworthy examples of chemical displacement, in the context of the present work, have been the application of bismuth (by Campbell and co-workers[28,29,48−50]) and the application of trimethylphosphine (by Muetterties, Friend, et al.[22−26]) as displacing agents to study the reactions of hydrocarbons on platinum and nickel single-crystal surfaces.

These prior experiments indicate how the phenomenon of chemical displacement can be applied to study surface chemistry and in some cases to extract kinetic information concerning the temperatures of elementary reaction steps on surfaces. In the present work we demonstrate the generality of the chemical displacement phenomenon for hydrocarbon adsorbates on copper surfaces and show how this process can be used as a tool for quantitative kinetic studies of decomposition and synthesis reactions on surfaces. A key feature of these studies is that the chemical displacement is carried out at low temperature, where the displaced molecules remain physisorbed on top of the monolayer of the displacing agent. Figure 1 illustrates such an idealized, low-temperature, chemical displacement process with two generic adsorbates, A and B, where A bonds more strongly to the surface than B. As shown, if the chemical displacement reaction is quite facile and the temperature of the surface is held low enough during this displacement process, then the displaced species, B, will remain adsorbed in a second layer or multilayer. The number of displaced molecules can then be quantified from the area of the desorption peak in a subsequent TPD experiment. Thus, if a surface chemical reaction is quenched by cooling to low temperature, the extent to which a displaceable reactant has been consumed or a displaceable

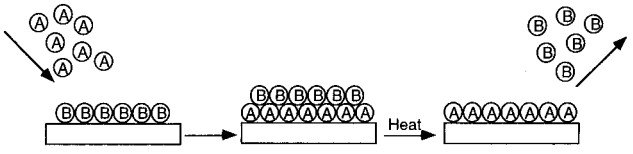

Figure 1. Schematic chemical displacement reaction in which species B, initially adsorbed in the first layer, is displaced to the second layer during the adsorption of impinging gas-phase species A. If the chemical displacement experiment is conducted at low temperature, the displaced B molecules will remain adsorbed in the second layer. When the surface in a temperature-programmed desorption experiment is heated, the B molecules will desorb from the surface at the multilayer desorption temperature.

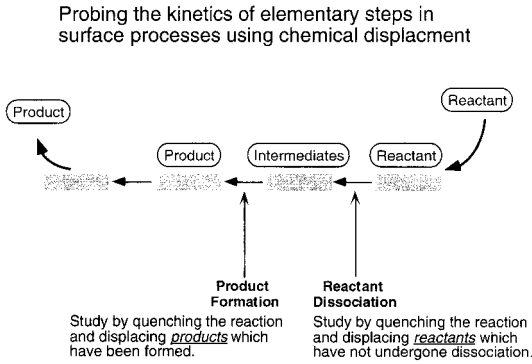

Figure 2. Schematic diagram of the kinds of adsorbate reactions that can be studied using chemical displacement. The kinetics of both bond dissociation and bond formation can be determined by applying chemical displacement following an anneal/quench cycle. The extent of reaction is quantified by detecting the displaced reactants or products that desorb in a subsequent temperature-programmed desorption experiment.

product has been formed can be quantitatively determined. Both of these applications (adsorbate decomposition and adsorbate synthesis) are indicated schematically in Figure 2 and are illustrated with the experiments described in the text below using the reactions of halogenated hydrocarbons on copper surfaces.

II. Experimental Section

The experiments were performed in ultrahigh vacuum (UHV) systems at Columbia University and Brookhaven National Laboratory. Details of the Columbia UHV chamber and of experimental protocol for TPD studies are presented in ref 52. Briefly, the Cu(100) and Cu(110) crystals (Monocrystals, 99.999%) were cleaned by cycles of Ar^+ sputtering and annealing. Reactants were adsorbed onto the crystal by backfilling the chamber. Cyclopentene (Aldrich, 99%), benzene (Fischer, 99.9%), iodobenzene (Aldrich, 99%), iodobenzene-d_5 (Icon, 97 atom. % D), and methyl iodide (Aldrich, 99.5%) were purified by several freeze−pump−thaw cycles with liquid nitrogen prior to dosing, and sample purities were confirmed in situ by mass spectrometry. Vinyl bromide, a gas (Matheson, 99.5%), was used as received, without further purification. All exposures are reported in Langmuirs (1 Langmuir (L) = 1×10^{-6} Torr s) and are uncorrected for differing ion gauge sensitivities. The quadrupole mass spectrometer (QMS) is installed behind a differentially pumped shield containing a 2 mm diameter aperture. In TPD studies, the sample was held 1−2 mm from the aperture so that only molecules evolved from the central portion of the 1 cm diameter crystal contribute to the detected signal. The heating rate in all TPD experiments was 3 K/s.

The near-edge X-ray absorption fine structure (NEXAFS) measurements were conducted on beamline U1 of the national synchrotron light source (NSLS) at Brookhaven National Laboratory. A detailed description of the experimental end station apparatus has been given in ref 53. The two-stage UHV chamber is equipped with an ion-sputtering gun, a quadrupole mass spectrometer, and an Auger electron spectrometer, which allowed confirmation that the desired vinyl bromide-covered surfaces were reproduced in this chamber. Control experiments on clean and vinyl bromide-precovered Cu(100) surfaces revealed that carbon monoxide and water adsorption from background gases ($P < 1 \times 10^{-9}$ Torr) had no detectable effect on the vinyl bromide NEXAFS spectra reported here. All spectra were recorded with a partial electron yield detector with a retarding voltage of −200 eV. The resolution of the synchrotron monochromator was set at 0.3 eV throughout the

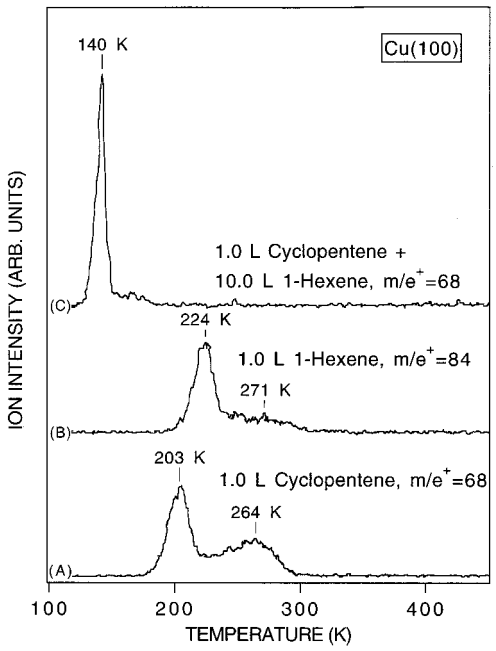

Figure 3. Temperature-programmed desorption spectra monitoring molecular desorption of (A) 1.0 L of cyclopentene at $m/e^+ = 68$ on Cu(100), (B) 1.0 L of 1-hexene at $m/e^+ = 84$ on Cu(100), and (C) cyclopentene at $m/e^+ = 68$ following sequential adsorption of 1.0 L cyclopentene and 10.0 L 1-hexene on Cu(100) at 100 K. The results in (C) indicate, as discussed in the text, that 1-hexene displaces pre-adsorbed cyclopentent from the monolayer to the multilayer on Cu(100).

studies reported here. All NEXAFS spectra reported have been divided by the spectra of a clean surface taken at the same incidence angle and by the ratio of the signals from a reference grid that measures the incident beam intensity simultaneously with the NEXAFS spectra. The validity of such a treatment has been discussed in detail previously.[54]

III. Results

III.1. Low-Temperature Chemical Displacement of Physisorbed Hydrocarbons on Cu(100) and Cu(110). To illustrate the phenomenon of low-temperature chemical displacement, which we will later use to determine adsorbate reaction kinetics, we consider first the displacement of one unreactive adsorbate, cyclopentene, by a more strongly binding adsorbate, 1-hexene, on a Cu(100) surface. Plots A and B of Figure 3 show TPD spectra, monitoring the molecular ion, for 1.0 L exposures of cyclopentene and 1-hexene on Cu(100). The cyclopentene molecular desorption spectrum, Figure 3A, has two peaks (203 and 264 K) that result from desorption from terrace sites at low temperature (203 K) and from desorption from defect sites at high temperatures (264 K). (These assignments are based on studies of sputtered and sputtered plus annealed surfaces that are presented elsewhere.[55]) Notice that the 224 K terrace desorption peak in the 1-hexene TPD spectrum in Figure 3B is 21 K higher than the analogous terrace desorption peak at 203 K for cyclopentene desorption from Cu(100). Assuming that there is no barrier for adsorption, this kinetic result indicates that 1-hexene bonds more strongly (in terms of free energy) to the Cu(100) surface than does cyclopentene. A first-order analysis, based on the peak desorption temperatures and assumed preexponential factors of 10^{13} s^{-1}, indicates that the activation energy for 1-hexene desorption (13.5 kcal/mol) is 1.2 kcal/mol higher than the activation energy for cyclopentene desorption (12.3 kcal/mol) from Cu(100). These results indicate a thermodynamic driving force for 1-hexene to displace cyclopentene

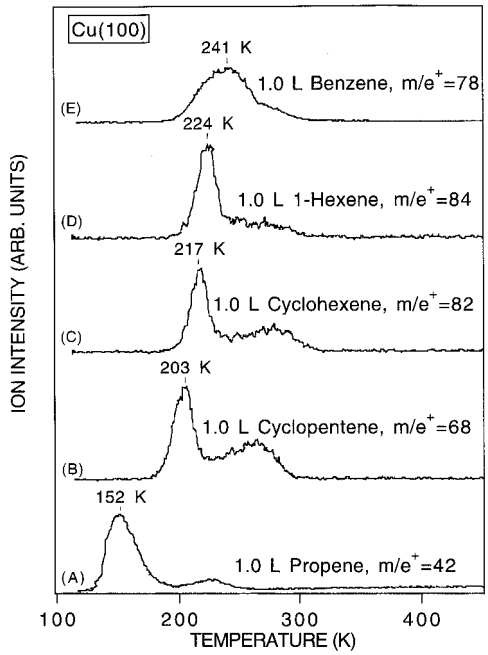

Figure 4. Temperature-programmed desorption spectra monitoring molecular desorption of 1.0 L of (A) propene at $m/e^+ = 42$, (B) cyclopentene at $m/e^+ = 68$, (C) cyclohexene at $m/e^+ = 82$, (D) 1-hexene at $m/e^+ = 84$, and (E) benzene at $m/e^+ = 78$ from Cu(100).

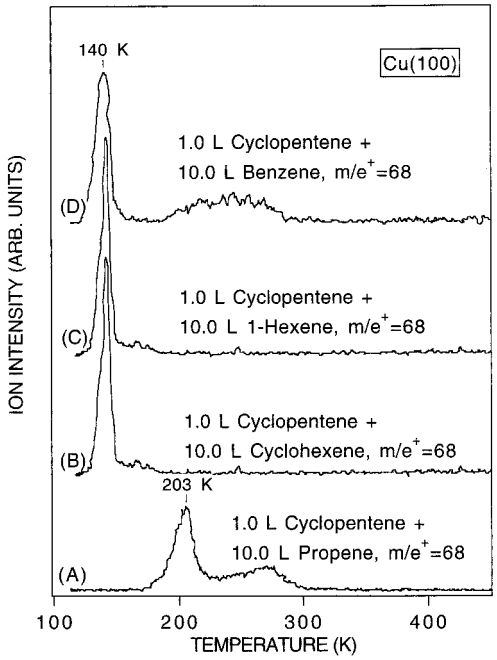

Figure 5. Temperature-programmed desorption spectra monitoring molecular desorption of cyclopentene at $m/e^+ = 68$ from Cu(100) following sequential adsorption of 1.0 L of cyclopentene and 10.0 L of (A) propene, (B) cyclohexene, (C) 1-hexene, and (D) benzene. The spectra indicate that cyclohexene, 1-hexene, and benzene, but not propene, can displace monolayer coverages of cyclopentene to the multilayer, where it desorbs at the 140 K multilayer desorption temperature.

from the monolayer on Cu(100). The kinetic facility of this process at 110 K is demonstrated by the results in Figure 3C.

Figure 3C shows TPD results for a cyclopentene-covered Cu(100) surface (the same 1.0 L exposure, 40% of ML saturation, as in Figure 3A) that has been exposed to 10.0 L (4.0 ML) of 1-hexene. Figure 3C, which plots the resulting TPD spectrum for the cyclopentene parent ion, $m/e^+ = 68$, shows that virtually all of the cyclopentene initially adsorbed on Cu(100) is evolved at 140 K (the same temperature at which cyclopentene multilayer desorption occurs) after exposure to the 1-hexene displacing agent. These results show that even a relatively small binding energy difference of approximately 1.0 kcal/mol is sufficient to displace weakly adsorbed molecules from the catalytically active monolayer sites. It is also clear that the displacement process is quite facile in this system, occurring at or below 140 K.

The generality of this displacement phenomenon for unsaturated, low-molecular weight hydrocarbons on Cu(100) is demonstrated by the results in Figures 4 and 5. These TPD studies illustrate the general finding that (for the representative series of benzene, 1-hexene, cyclohexene, cyclopentene, and propene) the adsorbate with the higher molecular desorption temperature, and consequently the larger free energy of adsorption in the monolayer, displaces the adsorbate with the lower adsorption free energy (i.e., lower molecular desorption temperature). Specifically, Figure 4 plots the TPD spectra (monitoring the molecular ions) that result when 1.0 L of each of these molecules is adsorbed separately on Cu(100). Again, each spectrum shows two peaks as a result of the different binding energies of these unsaturated hydrocarbons on the (100) terraces versus surface defect sites. As Figure 4 indicates, the desorption temperature is highest for benzene and decreases in the order 1-hexene > cyclohexene > cyclopentene > propene.

This sequence of binding energies suggests that benzene, 1-hexene, and cyclohexene (but not propene) will displace submonolayer coverages of cyclopentene on Cu(100). Figure 5 confirms this expectation. The TPD spectra in Figure 5 show molecular desorption of cyclopentene after a Cu(100) surface has been exposed to 1.0 L of cyclopentene followed by 10.0 L of propene (Figure 5A), cyclohexene (Figure 5B), 1-hexene (Figure 5C), and benzene (Figure 5D).

As expected, the 10.0 L exposures of benzene, 1-hexene, and cyclohexene all result in cyclopentene evolution at 140 K, which is the same (to within the ±5 K reproducibility of these experiments) as the temperature for desorption of cyclopentene adsorbed on top of monolayers of these displacing agents. Additionally, Figure 5A reveals that 10.0 L of propene fails to displace cyclopentene from monolayer sites. In this case, cyclopentene continues to desorb at the same 203 K peak temperature as observed for 1.0 L of cyclopentene adsorbed alone (i.e., Figure 5A is virtually indistinguishable from Figure 4B).

The results in Figure 5D above also show that little, if any, of the cyclopentene molecules that bind to defect sites, and desorb between 230 and 300 K, are displaced by the benzene molecules. This result is not surprising, since the cyclopentene molecules at defect sites have a larger binding energy (i.e., larger free energy of adsorption) compared to the benzene molecules at these sites. This finding suggests an interesting structure sensitivity for chemical displacement; i.e., benzene displaces cyclopentene from the Cu(100) terraces, but the reverse appears to be true for low-coordination-number defect sites. This structure sensitivity is substantiated by studies of a Cu(110) surface where even those surface atoms in the terraces have a coordination number of only 6 compared with 8 for the surface atoms on Cu(100). Figure 6 shows TPD spectra, monitoring the molecular ion, when 1.0 L of cyclopentene and benzene are dosed separately onto Cu(110). Notice that the desorption peak temperature for cyclopentene (Figure 6A) on Cu(110) is 262 K, while the desorption peak temperature for benzene (Figure 6B) is 240 K. Thus, while the benzene adsorption energy on Cu(110) is nearly identical with that presented above on Cu(100), cyclopentene bonds much more strongly on

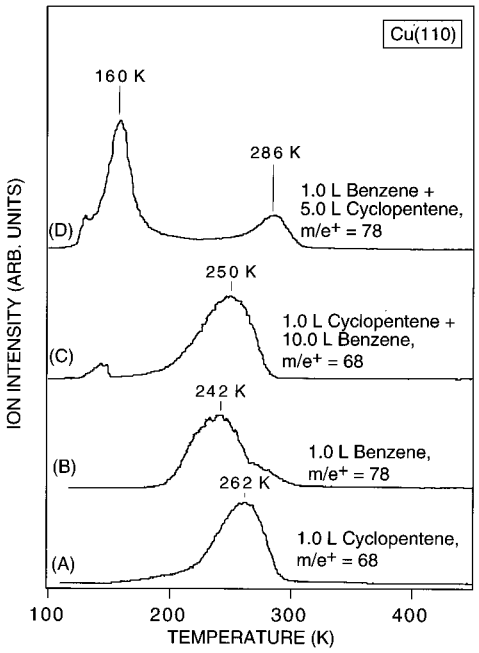

Figure 6. Temperature-programmed desorption spectra monitoring molecular desorption of (A) 1.0 L cyclopentene at $m/e^+ = 68$, (B) 1.0 L benzene at $m/e^+ = 78$, (C) cyclopentene at $m/e^+ = 68$ following sequential adsorption of 1.0 L of cyclopentene and 10.0 L of benzene, and (D) benzene at $m/e^+ = 78$ following sequential adsorption of 1.0 L of benzene and 5.0 L of cyclopentene on Cu(110). These spectra indicate that benzene cannot displace preadsorbed cyclopentene on Cu(110), even though benzene does displace cyclopentene on Cu(100) (see Figure 5). In addition, these spectra indicate that cyclopentene displaces a majority of preadsorbed benzene on Cu(110).

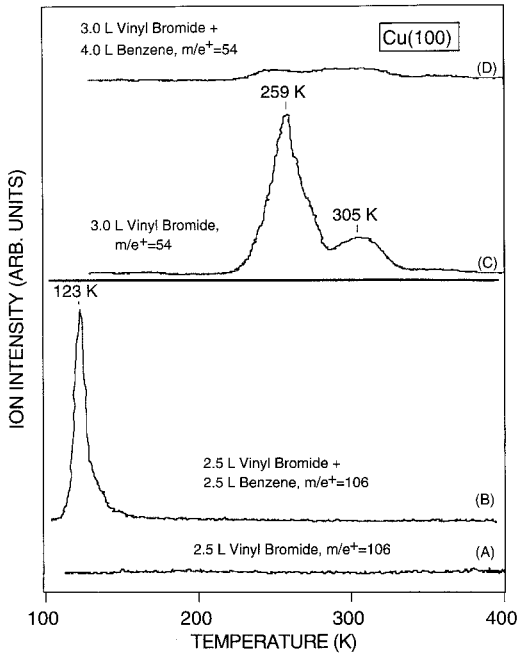

Figure 7. Temperature-programmed desorption spectra monitoring vinyl bromide molecular desorption at $m/e^+ = 106$, (A) and (B), or butadiene product desorption at $m/e^+ = 54$, (C) and (D), following (A) adsorption of 2.5 L vinyl bromide alone, (B) sequential adsorption of 2.5 L vinyl bromide and 2.5 L benzene, (C) adsorption of 3.0 L of vinyl bromide alone, and (D) sequential adsorption of 3.0 L vinyl bromide and 4.0 L benzene on Cu(100). These spectra indicate that benzene displaces 90% of a monolayer of preadsorbed vinyl bromide to the multilayer on Cu(100).

Cu(110) than on Cu(100). First-order analysis based on the desorption peak temperatures (with assumed preexponential factors of 10^{13} s^{-1}) indicate that the cyclopentene binding energy on Cu(110) is 1.4 kcal/mol greater than the benzene binding energy on the same Cu(110) surface. Thus, on the basis of energetic considerations, one would expect that benzene will *not* displace preadsorbed cyclopentene on Cu(110).

Figure 6C displays the TPD spectrum that results from attempting to displace 1.0 L of preadsorbed cyclopentene on Cu(110) with 10.0 L of benzene. The spectrum, which monitors the cyclopentene molecular ion, $m/e^+ = 68$, clearly shows that most (95%) of the preadsorbed cyclopentene molecules on Cu(110) remain in the monolayer, unaffected by the subsequent addition of benzene. By contrast, the TPD spectrum in Figure 6D shows that when 1.0 L (0.4 ML) of preadsorbed benzene is exposed to 5 L of cyclopentene, 73% of the preadsorbed benzene is displaced by cyclopentene to the multilayer where it desorbs at 160 K. It should be noted in conjunction with this result that 73% net displacement after multilayer desorption does not necessarily imply that 73% of the monolayer molecules are displaced to the second layer prior to desorption. Entropic factors and a dynamic equilibrium between the first and second layers as the surface is heated in the thermal desorption experiment can result in differences between the second-layer concentration at the 110 K adsorption temperature and the second-layer desorption yields. This issue is quantitatively addressed in section IV. In any event, most of the benzene molecules on Cu(110) are displaced and desorbed from the monolayer by cyclopentene during a TPD experiment.

Despite the obvious steric issues in getting one molecule to slide under another at an interface, it is clear from the results above as well as from those in Tables 1−3 that chemical displacement processes tend to be quite facile and common for a wide range of adsorbates and interfaces. In addition, the comparison above of Cu(110) and Cu(100) surfaces, where the ability of benzene and cyclopentene to displace each other is reversed, emphasizes the specificity of displacement process to the details of the system, including the atomic geometry of the surface. One molecule will not necessarily displace another molecule on all surfaces of the same metal or under all coverage conditions.

III.2. Determining Bond Dissociation Temperatures with Chemical Displacement. Having established the chemical displacement phenomenon for hydrocarbon monolayers on Cu(100), we now illustrate the application of chemical displacement to study the kinetics of bond dissociation, specifically C−Br bond dissociation in vinyl bromide adsorbed on Cu(100). When Cu(100) surface is exposed to vinyl bromide, the first monolayer adsorbs irreversibly. As described in detail elsewhere,[56] a 2.5 L exposure corresponds to a monolayer of vinyl bromide and, as shown in Figure 7A, no molecular desorption (as monitored by the parent ion at $m/e^+ = 106$) is detected in the absence of a displacing agent for a monolayer exposure. The studies in ref 56 show that the absence of molecular desorption from the monolayer is a result of vinyl bromide dissociation on Cu(100) to form vinyl groups that subsequently couple near 250 K with 100% selectivity to form butadiene. The evolution of this coupling product is shown by the $m/e^+ = 54$ TPR/D (temperature-programmed reaction/desorption) curve in Figure 7C. The purpose of the current work is merely to demonstrate the effectiveness of chemical displacement for determining the C−Br bond dissociation temperature.

As the previous section emphasized, the first step in a successful chemical displacement experiment is choosing a suitable displacing agent. The data in Figure 7 show that benzene displaces 90% of a vinyl bromide monolayer from Cu(100). This conclusion was reached by comparing TPD spectra (monitoring vinyl bromide molecular desorption and

butadiene formation) with and without the addition of benzene as a displacing agent. Figure 7A shows that a 2.5 L exposure of vinyl bromide alone results in no molecular desorption in the subsequent TPD experiment, but as shown in Figure 7B, the addition of a 2.5 L exposure of benzene to a 2.5 L exposure of vinyl bromide results in significant vinyl bromide molecular desorption at the 123 K multilayer desorption temperature. The multilayer vinyl bromide molecular desorption in Figure 7B results because benzene displaces vinyl bromide molecules from the monolayer to the multilayer where they can no longer interact with and dissociate on the Cu(100) surface.

Although the results in Figure 7B indicate that benzene can displace some portion of a vinyl bromide monolayer from Cu(100), they do not determine the extent of displacement. To determine the fraction of vinyl bromide molecules that are displaced by benzene, experiments directly analogous to those shown in parts A and B of Figure 7 have been performed while monitoring the $m/e^+ = 54$ butadiene produced by the vinyl coupling reaction. Comparison of the butadiene yields with and without displacement by benzene (parts C and D of Figure 7) indicates that the addition of benzene as a displacing agent results in a 90% reduction in the amount of butadiene product. This decreased yield reflects displacement of the vinyl bromide molecules to the multilayer before they dissociate to produce the vinyl fragments that would have coupled to form butadiene. As a result of this facile displacement, benzene has been applied as the displacing agent in experiments (described below) that determine the vinyl bromide C−Br bond dissociation temperature.

Determination of the C−Br bond dissociation temperature in vinyl bromide with chemical displacement is possible because vinyl bromide can only be displaced to the multilayer as long as it remains molecularly intact. Once the temperature of the surface is high enough, the vinyl bromide irreversibly dissociates, producing vinyl groups and bromine atoms, which are not displaced by benzene. Consequently, the scheme employed is to cover the surface with 1 ML of vinyl bromide at 110 K and then to anneal the surface to a certain temperature. After the reaction is quenched by cooling back to 110 K, the surface is exposed to 2.5 L (1 monolayer) of the benzene-displacing agent. If the vinyl bromide anneal temperature was insufficient to dissociate the C−Br bond, the vinyl bromide will remain molecularly intact, and will be displaced to the multilayer by benzene, and detected in the subsequent TPD measurement. On the other hand, if the vinyl bromide anneal temperature was sufficiently high to dissociate all of the vinyl bromide, there will be no remaining molecularly intact vinyl bromide when the benzene displacer is added, and no vinyl bromide will be detected in the subsequent TPD measurement. The yield of displaced vinyl bromide as a function of surface anneal temperature, therefore, provides a direct measure of the extent of the vinyl bromide dissociation reaction.

The filled circles in Figure 8 plot the vinyl bromide molecular ion TPD spectrum peak area as a function of the temperature to which the surface is annealed after vinyl bromide exposure at 110 K and before exposure to the benzene-displacing agent. (The TPD spectra corresponding to the data in Figure 8 are presented elsewhere.[56]) As shown, increasing the vinyl bromide anneal temperature decreases the yield in the vinyl bromide molecular ion TPD spectra with virtually no vinyl bromide yield when the surface is warmed to 187 K where all the vinyl bromide has dissociated. The inflection point in the fit to the vinyl bromide yield as a function of anneal temperature plot, which occurs at 157 K, reflects the temperature where the rate of dissociation of vinyl bromide molecules is the largest, just as the temperature of the peak maximum in a TPD spectrum reflects the temperature at which the rate of desorption from the surface is largest.

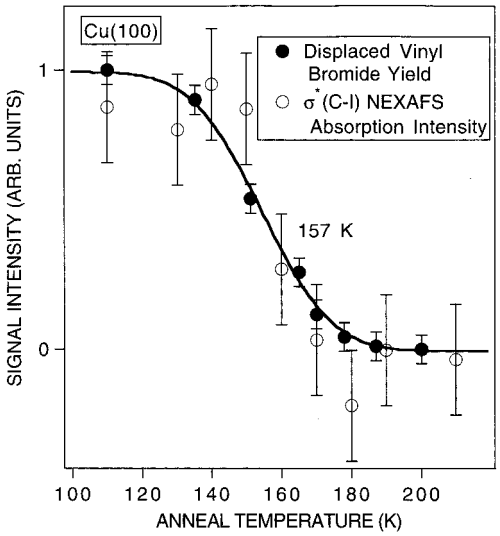

Figure 8. Results of spectroscopic studies (○) and chemical displacement studies (●) to determine the C−Br bond dissociation temperature in vinyl bromide on Cu(100). In each of these sets of experiments, a 2.5 L exposure of vinyl bromide was briefly annealed to the temperature indicated and the fraction of unreacted vinyl bromide remaining on the surface was then determined. In the chemical displacement studies, the amount of unreacted vinyl bromide was quantified by thermal desorption after displacement by a 2.5 L exposure of benzene. In the NEXAFS spectroscopy studies, the amount of unreacted vinyl bromide was quantified from the intensity of the n(C1s) → σ^*(C−Br) transition. The solid line is a fit to the TPD yield. As discussed in the text, both experiments indicate that the C−Br bond in vinyl bromide dissociates with a maximum rate near 157 K. (The large error bars on the NEXAFS peak intensities, and the negative value of the data point obtained after annealing to 180 K, reflect the relatively small signal-to-noise ratio in these spectra.)

To determine the accuracy and validity of using chemical displacement to determine bond dissociation temperatures, we compare the results above with the vinyl bromide dissociation temperature determined using near-edge X-ray absorption fine structure (NEXAFS) spectroscopy. Complete details of these NEXAFS results will appear elsewhere.[56] Here, we present only those details necessary to determine the C−Br bond dissociation temperature. The pertinent feature in the near-edge fine structure of the carbon K-edge spectra is the n(C_{1s}) → σ^*(C−Br) absorption feature at 287.5 eV. The intensity of this n(C_{1s}) → σ^*(C−Br) resonance is directly proportional to the number of undissociated C−Br bonds on the Cu(100) surface. The open circles in Figure 8 plot the intensity of this n(C_{1s}) → σ^*(C−Br) absorption as a function of surface anneal temperature for a Cu(100) surface exposed to 2.5 L of vinyl bromide at 95 K. These intensities provide a direct measure of the extent of C−Br bond dissociation as a function of surface temperature. (The magnitudes of the filled circles in Figure 8 were determined by normalizing the n(C_{1s}) → σ^*(C−Br) peak intensity to the difference between the intensity of the preedge and the carbon-K postedge in each NEXAFS spectrum. The scatter in these n(C_{1s}) → σ^*(C−Br) peak intensities and the negative value for the data point obtained after annealing to 180 K reflect the small signal-to-noise levels in these experiments.) As Figure 8 indicates, after annealing to 210 K there is no intensity in the n(C_{1s}) → σ^*(C−Br) absorption feature, indicating dissociation of all vinyl bromide C−Br bonds below this temperature. The temperature at which the rate of dissociation of vinyl bromide is largest, as determined by the inflection point in the fit to the n(C_{1s}) → σ^*(C−Br) absorption intensity vs surface temperature,

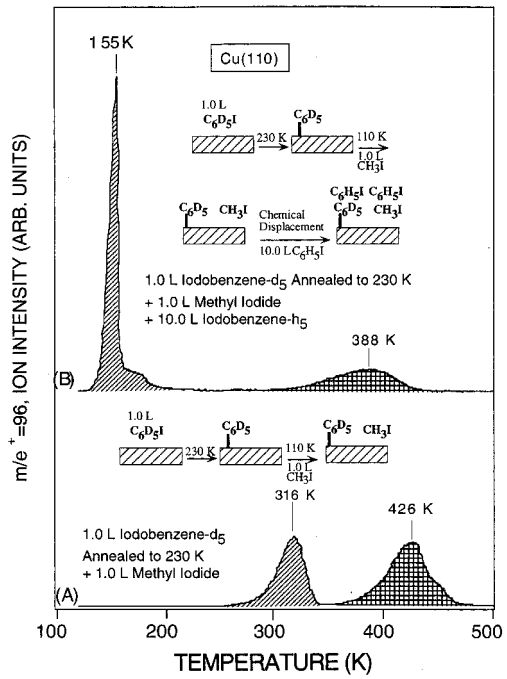

Figure 9. Temperature-programmed desorption spectra monitoring toluene-d_5 evolution at $m/e^+ = 96$ following (A) addition and (B) no addition of 10.0 L of iodobenzene-d_5 to a Cu(110) surface that had been previously exposed to 1.0 L of iodobenzene-d_5, annealed to 230 K, and then exposed to 1.0 L of methyl iodide.

is 158 K. Although this fit to the $n(C_{1s}) \rightarrow \sigma^*(C-Br)$ absorption intensity is not shown in Figure 8, it is virtually indistinguishable from the fit to the displaced vinyl bromide TPD yield, which is also depicted in Figure 8.

The chemical displacement experiments described above, which determined significant vinyl bromide C−Br bond dissociation on Cu(100) between 140 and 170 K with the rate of dissociation of vinyl bromide molecules peaking at 157 K, agree very well with these NEXAFS results. This comparison indicates that the chemical displacement provides a simple, economical, and accurate method of determining bond dissociation temperatures of adsorbates on metal surfaces.

III.3. Determining Adsorbate Coupling Reaction Temperatures With Chemical Displacement. To demonstrate the utility of chemical displacement for determining not only the temperature of an adsorbate coupling reaction but also the mechanism of that reaction, we examine the reaction of methyl iodide with adsorbed phenyl groups on Cu(110). Since a detailed discussion of this reaction will be given elsewhere,[57] this section presents only the material necessary to understand the reaction kinetics as determined by chemical displacement.

When submonolayer coverages of phenyl groups on Cu(110) (generated by dosing 1.0 L of iodobenzene-d_5 at 95 K and briefly annealing the surface to 200 K to break the C−I bond) are exposed to 1.0 L of methyl iodide at 95 K, the subsequent TPD spectrum, shown in Figure 9A, shows two distinct channels for the formation of toluene product. The high-temperature channel with a peak at 426 K results from coupling of chemisorbed methyl and chemisorbed phenyl groups followed by immediate product desorption. This high-temperature reaction-limited toluene formation channel has been previously described[58] and will not be discussed further. The reaction mechanism for the low-temperature toluene formation channel, with a peak desorption temperature of 316 K in Figure 9A, is less obvious. Since the product formed by this low-temperature channel desorbs at the same 316 K temperature as a similar coverage of molecular toluene on an otherwise clean Cu(110) surface, the evolution of toluene at 316 K in Figure 9A is probably desorption-limited. In other words, the coupling reaction to form toluene probably occurs below 316 K and the product toluene remains bound to the surface until 316 K where it desorbs. In particular, it is possible that toluene is formed concurrently with C−I bond dissociation in methyl iodide, which occurs at approximately 140 K on clean Cu(100).[59,60] Such a result would be highly suggestive of a direct reaction between methyl iodide and coadsorbed phenyl groups, possibly even indicating a pathway involving a methyl radical intermediate, since methyl radical evolution has been previously detected concurrently with C−I bond scission in methyl iodide on Cu(100).[59,60] The chemical displacement results presented below place an upper limit on the temperature for the low-temperature phenyl−methyl coupling pathway.

The kinetics of the coupling reaction between phenyl and methyl have been studied by employing chemical displacement of the product toluene molecules. In this case, after generating a low coverage of deuterated phenyl groups (C_6D_5) on the Cu(110) surface and dosing 1.0 L of methyl iodide, the surface was exposed to 10.0 L of iodobenzene, C_6H_5I, as a displacing agent for toluene. Though not shown here, we have determined that iodobenzene quantitatively displaces 100% of a monolayer of toluene to the multilayer. The TPD spectrum in Figure 9B shows that following addition of the iodobenzene-displacing agent, the low-temperature toluene channel (which appeared at 316 K in the absence of a displacing agent) is now observed at the 155 K multilayer desorption temperature.

The results of the toluene product displacement experiment in Figure 9B show the evolution of displaced toluene at 155 K even when the surface is not annealed between dosing methyl iodide and adding the iodobenzene-displacing agent, which is suggestive of reaction at the 95 K methyl iodide adsorption temperature. In fact, however, these results only determine that coupling of phenyl with methyl occurs below the 155 K toluene evolution temperature, since the excess iodobenzene-displacing agent in the multilayer does not desorb until 160 K. As a result, any product toluene formed below 160 K will be displaced by the second-layer iodobenzene. Such displacement during the TPD heating ramp would not be an issue if the second-layer iodobenzene also displaced the reactant methyl iodide, but it has been found that iodobenzene cannot displace methyl iodide from the monolayer to the multilayer for the low methyl iodide coverages used in these experiments. Consequently, it is possible that unreacted molecular methyl iodide and phenyl groups remain in the monolayer even after the iodobenzene has been added as a displacing agent to the surface. In this case, the iodobenzene would simply fill multilayer sites at 95 K. As long as the phenyl−methyl coupling reaction occurs below the 160 K iodobenzene desorption temperature, the product toluene will be displaced (by iodobenzene, which was initially in multilayer sites) from the monolayer to the multilayer, where it can desorb at 155 K as shown in Figure 9B.

This study thus indicates both the potential and the limitations in applying chemical displacement to monitor surface reactions. The limitations concern low-temperature reactions that occur at or below the temperature of desorption of the displacing agent from the multilayer, since in this case the presence or absence of displaced products at the multilayer desorption temperature provides only an upper limit for the temperature of reaction. In other words, regardless of whether reaction has occurred prior to desorption of the displacing agent from the multilayer or simultaneously with it, a temperature-programmed desorption sweep will give exactly the same result, and so only an upper limit can be placed on the temperature of such a reaction. On

the other hand, most surface reactions will occur at temperatures significantly above that for multilayer desorption, in which case the major requirement for measuring the kinetics of reactant dissociation or product formation is the ability to displace the reactants and products from the monolayer at low temperatures. In the present study only an upper limit of 155 K can be placed on the coupling reaction, and the similarity of this temperature to that for methyl iodide C−I bond dissociation suggests, as detailed in a forthcoming publication,[57] that the reaction involves a methyl radical, which is produced in the Cu(110)-catalyzed dissociation of methyl iodide and which reacts with coadsorbed phenyl before bonding to the Cu(110) surface.

IV. Discussion

The results presented above indicate that low-temperature chemical displacement of a weakly binding adsorbate by a more strongly binding hydrocarbon on copper surfaces is quite facile. In addition, these experiments demonstrate that chemical displacement can be successfully used to determine both the adsorbate bond dissociation temperature in vinyl bromide adsorbed on Cu(100) and the C−C bond formation temperature in the reaction of coadsorbed phenyl plus methyl iodide on Cu(110). This application of chemical displacement to determine the kinetics of the reactions of adsorbed molecules is similar to previous experiments by Muetterties, Friend, et al.[22−26] using trimethylphosphine as a displacing agent and by Campbell and co-workers[28,29,48−50,61] using BPTDS (bismuth-postdosing thermal desorption spectroscopy). In the present experiments, however, the use of low-temperature chemical displacement, followed by TPD, allows quantitative determination of the yield of displaced reactant or product.

Since the present results probe the desorbing displaced molecules in a TPD experiment, they do not directly address the question of whether the actual displacement occurs at the adsorption temperature or during the subsequent TPD experiment. An examination of previous displacement experiments along with an investigation of the thermodynamics of chemical displacement, however, can address this question. For example, previous experiments using surface sensitive vibrational spectroscopies to study isotopic exchange of C_6H_6 and C_6D_6 between adsorbed layers on Ru[18,19] and Cu[20] provide evidence of chemical displacement at the 110 K adsorption temperature. In addition, previous X-ray diffraction experiments have determined that the displacement of Kr,[45] C_6H_{12},[46] and CCl_4[47] by Xe occurs on graphite at approximately 80 K. These previous results, then, suggest that some chemical displacement probably occurs at the 100 K adsorption temperature used in the present experiments. These previous experiments, however, do not address the extent to which the second-layer population of displaced molecules determined by the TPD desorption yield reflects the actual second-layer population at the 100 K adsorption temperature. In other words, some displacement might occur at 100 K, but the extent of displacement may change as the surface temperature is increased during a TPD experiment. To address this issue, a discussion of the thermodynamics of the chemical displacement process must now be presented.

The results above, as well as many of the previous results listed in Tables 1−3, suggest that these chemical displacement processes achieve thermodynamic equilibrium in the few seconds between adding the displacing agent and the beginning of the TPD experiment. Because equilibrium is probably achieved on a time scale that is fast compared to the time scale of the TPD experiment, thermodynamics is probably the determining factor in the extent of displacement and in the characteristics of the displacement TPD spectra. Since the equilibrium configuration of the initial adsorbate and displacing agent minimizes the Gibbs free energy, either entropy or enthalpy could provide the driving force for displacement.

One can write the changes in the Gibbs free energy upon displacement as

$$\begin{aligned} dG_{DISP} &= \sum_{i,j} \mu_{i,j}\, dn_{i,j} \\ &= \sum_{i,j} (\mu_{i,j}^{\circ} + RT \ln(n_{i,j}))\, dn_{i,j} \\ &= \sum_{i,j} (h_{i,j}^{\circ} - Ts_{i,j}^{\circ} + RT \ln(n_{i,j}))\, dn_{i,j} \end{aligned} \quad (1)$$

where $\mu_{i,j}$ is the chemical potential of the ith component of the system in the jth layer (for the system described here $i,j = 1$ or 2), $n_{i,j}$ is the mole fraction of the ith component in the jth layer, $h_{i,j}^{\circ}$ is the standard enthalpy for the ith component being in the jth layer, and $s_{i,j}^{\circ}$ is the standard entropy for the ith component being in the jth layer. In eq 1 the term in $R \ln(n_{i,j})$ may be identified as the entropy of mixing. This contribution to the entropy is always present, even when the absolute entropy terms ($s_{i,j}^{\circ}$) cancel ($\sum_{i,j} s_{i,j}^{\circ} = 0$) as assumed below.

Equation 1 gives for the equilibrium condition $dG_{DISP} = 0$:

$$-RT \ln(K) = \Delta G^{\circ}_{DISP} = \sum_{i,j} h_{i,j}^{\circ} - T \sum_{i,j} s_{i,j}^{\circ} \quad (2)$$

where K is the equilibrium constant and ΔG°_{DISP} is a change in standard Gibbs free energy upon displacement. Given the similarity in molecular structure between the molecules being displaced and those doing the displacing, it is reasonable to presume that the changes in absolute entropies for the two species during displacement are equal in magnitude and opposite in sign so that $\Delta S^{\circ}_{DISP} = \sum_{i,j} s_{i,j}^{\circ} \approx 0$. Thus, we can equate ΔH° for displacement with ΔG° for displacement, which in turn gives the equilibrium layer concentrations for the displacement process. Furthermore, because the systems investigated here are all weakly bound hydrocarbons, ΔH_{DISP} is not expected to be highly temperature- or coverage-dependent. Therefore, we take ΔH_{DISP} as ΔH°, which, given the approximations above, is equal to ΔG°.

When the enthalpy change for displacement is determined, changes in both adsorbate−adsorbate and adsorbate−surface interactions must be considered. If, however, we assume that the enthalpy of mixing within each of the individual layers during the displacement process is zero, then adsorbate−adsorbate interactions can be neglected and one can define the change in enthalpy upon displacement, ΔH_{DISP}, in terms of experimental observables in the TPD spectra. Up to this point, it has been tacitly assumed that the dominant adsorbate−surface interaction is the adsorbate−metal binding energy. The change in enthalpy upon displacement, however, depends also on the second-layer binding energies as demonstrated by the thermodynamic cycle in Figure 10. As this cycle shows, the enthalpy change for complete displacement of species B by species A is given by the sum of the enthalpies for desorbing A and B from the second layer and monolayer, respectively, plus the enthalpies for adsorbing A and B onto the monolayer and second layer, respectively. Mathematically,

$$\Delta H_{DISP} = [(\Delta H_{1B}) + (\Delta H_{2A})] + [(-\Delta H_{1A}) + (-\Delta H_{2B})] \quad (3)$$

(Although enthalpy changes upon adsorption are negative, the convention within the community is to define the enthalpy of

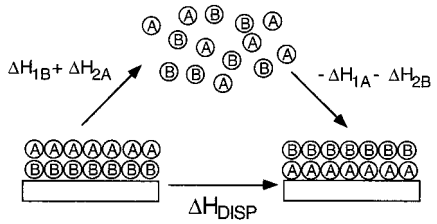

Figure 10. Thermodynamic cycle for the chemical displacement of one layer of species A by one layer of species B. Using the system with both species removed to the gas phase as an intermediate in the displacement cycle reveals that the change in enthalpy upon displacement is $[(\Delta H_{1B}) + (\Delta H_{2A})] + [(-\Delta H_{2B}) + (-\Delta H_{1A})]$. The individual enthalpy terms, ΔH_{1A}, etc., are the heats of adsorption of the A or B species in the first or second layer as discussed in the text. (The addition of negative signs in front of the individual enthalpy terms is to reconcile sign conventions for heats of adsorption with thermodynamic definitions as discussed in the text.)

adsorption, ΔH_{1A}, etc., as positive. Equation 3 maintains the conventional definition of a positive enthalpy of adsorption, with negative signs being inserted to reconcile this convention with the thermodynamic definition.) Equation 3 can be rewritten as

$$\Delta H_{DISP} = [\Delta H_{1B} - \Delta H_{2B}] - [\Delta H_{1A} - \Delta H_{2A}] \qquad (4)$$

in order to cast the enthalpy of displacement in molecule-specific terms. In other words, the terms in brackets are simply the differences in the heats of adsorption in the first and second layers. Thus, one can measure and tabulate differences between first- and second-layer heats of adsorption, and the larger the difference, the greater the displacing ability of the species.

Each of these individual enthalpies of adsorption can be determined from the desorption profiles in a TPD experiment. For example, the TPD spectra in Figures 3−5 indicate that for 1-hexene displacing cyclopentene on Cu(100), $\Delta H_{1A} = 13.5$ kcal/mol, $\Delta H_{2A} = 8.8$ kcal/mol, $\Delta H_{1B} = 12.3$ kcal/mol, and $\Delta H_{2B} = 8.4$ kcal/mol. The total change in enthalpy upon displacement of cyclopentene by 1-hexene on Cu(100), then, is −0.8 kcal/mol. The results of the chemical displacement experiments in Figures 3 and 5, which show that 1-hexene displaces virtually all of the monolayer cyclopentene molecules adsorbed on Cu(100), indicate that this −0.8 kcal/mol change in enthalpy upon displacement is enough to overcome the tendency toward random mixing of the two molecules between the first and second layers.

As was suggested above, the equilibrium mole fractions of first- and second-layer molecules as a function of temperature and the enthalpy change for displacement can be determined from $\Delta H^\circ_{DISP} \approx \Delta G^\circ = -RT \ln K$. Figure 11 plots the mole fraction of the displacing agent in the first layer, n_{1A}, as a function of ΔH°_{DISP} for several different surface temperatures. For reference, $n_{1A} = 1.0$ indicates complete displacement of B by A and $n_{1A} = 0.5$ indicates random mixing of A and B between the two layers. The results in Figure 11 confirm our intuitive expectations concerning the extent of displacement in the limits of small ΔH_{DISP} and large ΔH_{DISP}. For example, for all four temperatures shown, $\Delta H_{DISP} = 0$ results in $n_{1A} = 0.5$. Returning momentarily to eq 1, we see that this corresponds to

$$dG_{DISP} = RT \sum_{i,j} \ln(n_{i,j})\, dn_{i,j}$$

(since we have assumed that the terms in $s_{i,j}^\circ$ cancel), showing that the free energy of displacement is due solely to the terms in $R \ln(n_{i,j})$, which we have identified above with the entropy of mixing. Thus, the equilibrium point is set completely by this mixing term, which is essentially an entropic-driven

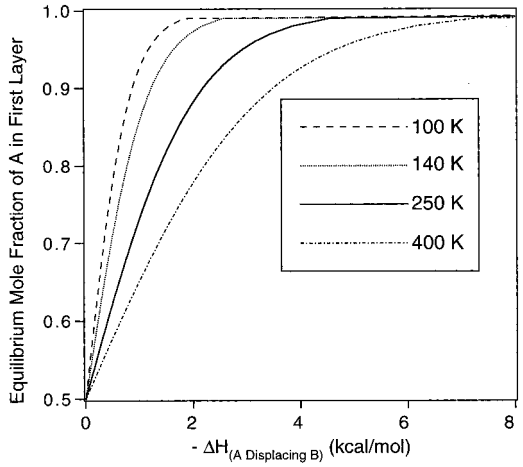

Figure 11. Mole fraction of species A in the first layer at thermodynamic equilibrium for a system prepared by coadsorbing one monolayer of species B and one monolayer of A, as a function of the change in enthalpy upon displacement of B by A at several different surface temperatures.

randomization of the adsorbate and the displacing agent between the two layers ($\Delta G^\circ_{DISP} = 0$, $K = 1$). At the other extreme, when ΔH_{DISP} is large (e.g., less than −2.0 kcal/mol), one finds complete displacement (i.e., $n_{1A} = 1$) at 100 K. As the surface temperature is increased, the mixing term, which scales with T, becomes more important, and at 400 K, complete displacement requires $\Delta H_{DISP} \simeq 8.0$ kcal/mol. In general, one finds that >99% displacement requires $|\Delta H_{DISP}/T| > 20$ cal/(mol K).

Of more direct relevance to the present experiment, Figure 11 also provides a prediction for the extent of displacement of cyclopentene by 1-hexene on Cu(100) where $\Delta H_{DISP} \approx -0.8$ kcal/mol. For a 100 K surface temperature, this simple calculation predicts a mole fraction of 1-hexene in the first layer of 0.9, or displacement of 90% of the initial cyclopentene molecules to the second layer. At 140 K, which is closer to the actual cyclopentene second-layer desorption temperature in Figure 3C, Figure 11 predicts displacement of 81% of the initial cyclopentene molecules to the second layer.

Although thermodynamics predicts displacement of a majority of monolayer cyclopentene by 1-hexene on Cu(100), it does not predict the nearly 100% displacement measured in the TPD experiment in Figure 3C. This lack of complete agreement with experiment likely results from the fact that the calculation assumes a static configuration of one monolayer of cyclopentene and one monolayer of 1-hexene. In the actual TPD experiment, the total number of adsorbed cyclopentene molecules decreases as the temperature is increased to near 140 K owing to desorption of displaced, second-layer cyclopentene. As the total number of adsorbed cyclopentene molecules decreases during the TPD experiment, the mole fraction of cyclopentene and 1-hexene in each layer must change to continually minimize the system's Gibbs free energy. Intuitively, as cyclopentene desorbs from the second layer, more first-layer cyclopentene should be displaced (law of mass action).

To address the extent of dynamic displacement of first-layer cyclopentene as second-layer cyclopentene desorbs during the TPD experiment, the displacement equilibrium has been analyzed for the case where a different total number of cyclopentene molecules are available for displacement from the first layer, thereby simulating the effect of removal of the adsorbate through the second-layer thermal desorption channel. Figure 12 plots the coverage of B (the species to be displaced) remaining in the first layer as a function of the total coverage (first and second layers) for three separate ΔH_{DISP} values, including $\Delta H_{DISP} =$

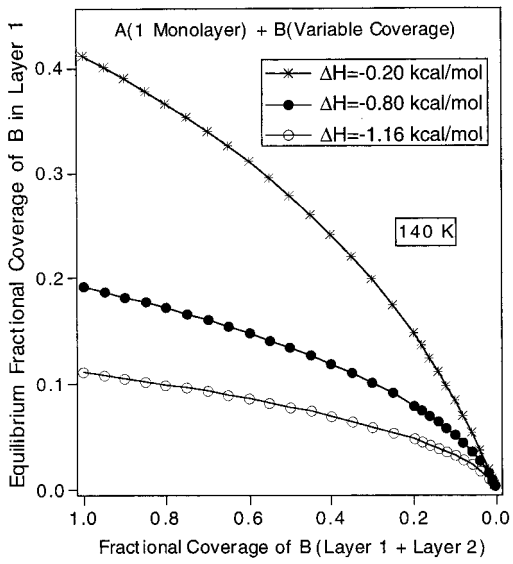

Figure 12. Coverage of species B in the first layer at thermodynamic equilibrium at 140 K for a system prepared by coadsorbing the indicated coverage of B and one monolayer of species A, as a function of total coverage of B in the first and second layers. The three separate curves are for the indicated changes in enthalpy upon displacement of B by A.

−0.8 kcal/mol, which applies for the case of 1-hexene displacing cyclopentene on Cu(100). The calculation is performed as follows. First, the equilibrium constant, K, is computed from $-\Delta H°_{DISP} = RT \ln K$. Then this equilibrium constant is used to calculate $[B_1]$ as a function of $([B_1] + [B_2])$. For $A_1 + A_2 = 1$ and $(B_1 + B_2)/(A_1 + A_2) = q$, the fraction of B in the first layer is given by $q - x$, with $x = B_2/(A_1 + A_2)$, where $x = \{-(1 + q)K \pm [K^2(1 + q)^2 + 4Kq(1 - K)]^{1/2}\}/[2(1 - K)]$. Consistent with the results in Figure 11, Figure 12 indicates that when no B has desorbed (i.e., total coverage of $B = B_1 + B_2 = 1$) and $\Delta H_{DISP} = -0.8$ kcal/mol, 19% of B remains in the monolayer. As the total coverage of B decreases, the fractional coverage of B in the first layer also decreases. This decrease in first-layer concentration of B results from the fact that B is displaced to the second layer to continually minimize the system's Gibbs free energy. After 80% of B has desorbed at 140 K, the fraction of B in the first layer has decreased to 8%. Note that as the coverage of B approaches zero, the fraction of B in the first layer also approaches zero so that it is possible for B to be selectively desorbed despite significant mixing between layers prior to and during desorption.

Consequently, Figure 12 suggests that even though only 81% of the initially adsorbed molecules are displaced when $\Delta H_{DISP} = -0.8$ kcal/mol and a full monolayer of both the initial adsorbate and the displacing agent are adsorbed on the surface, dynamic displacement during the TPD experiment can result in nearly 100% displacement of the initial adsorbate. This analysis assumes that all of the species displaced to the second layer desorb before any significant desorption of the second-layer displacing agent commences. In the case of cyclopentene displacement by 1-hexene on Cu(100), this assumption is justified by the 10 K higher second-layer desorption temperature for 1-hexene. Furthermore, the results in Figure 12 also suggest that even under less favorable displacement conditions (e.g., ΔH_{DISP} of only −0.2 kcal/mol) this dynamic displacement mechanism can still result in nearly total displacement of an adsorbate from the monolayer. In this case, even though 41% of the adsorbates initially in the monolayer remain in the first layer before any second-layer desorption occurs, all of the adsorbates initially in the monolayer are predicted to be displaced as second-layer molecules desorb during the TPD experiment.

Although this simple approach explains the results of the experiments presented here, in other systems adsorbate−adsorbate interactions and absolute entropy factors (situations where the terms in $s_{i,j}°$ do not cancel) may be much more important and may ultimately determine the efficiency and selectivity of chemical displacement. The success in explaining the present chemical displacement experiments based solely on first- and second-layer adsorbate binding energies results because we have specifically chosen systems in which there is a substantial difference between the initial adsorbate−metal binding energy and the displacer−metal binding energy. In systems where that binding energy difference is smaller, adsorbate−adsorbate interactions between the displacing agent and the initial adsorbate could easily alter the bonding to the metal surface sufficiently to affect the selectivity of the displacement reaction. Also, when the difference in binding energies to the surface is small, absolute entropy ($s_{i,j}°$) effects will contribute more significantly. For example, benzene, C_6H_6, and its deuterated isotope, C_6D_6, mix randomly between the monolayer and the multilayer on Cu(111).[20]

Finally, we re-emphasize a possible shortcoming in applying chemical displacement to determine reaction temperatures on surfaces. In an ideal displacement experiment, the displacing molecule should quantitatively displace the desired adsorbate from the monolayer to the multilayer. In addition, the reaction of interest should occur at a temperature higher than the temperature at which the displaced molecule desorbs from the multilayer. When both of these conditions are met, as in the example of C−Br bond dissociation in vinyl bromide on Cu(100), chemical displacement provides a simple means of determining reaction temperatures. When these two conditions are not met, however, the results of the chemical displacement experiment can be ambiguous as in the case of phenyl−methyl coupling on Cu(100), which was described in section III.3. In this system, because the reaction occurs below the temperature at which the displacing agent desorbs from the multilayer and because the displacing agent does not quantitatively displace the reactant CH_3I, we can conclude only that the coupling reaction must occur below 155 K, the temperature at which the displaced product toluene molecules desorb from the surface.

V. Conclusions

The experiments presented here demonstrate that chemical displacement can be quite facile at temperatures as low as 100 K and that low-temperature chemical displacement can be used as a simple and economical method for determining the kinetics of reactions occurring on surfaces under UHV conditions. In connection with the former, it was demonstrated that enthalpy is the driving force behind the displacement of cyclopentene by more strongly binding benzene, 1-hexene, and cyclohexene on Cu(100). In addition, surface structure sensitivity in chemical displacement has been demonstrated through studies showing that benzene displaces cyclopentene on Cu(100), while the reverse is true on Cu(110). Applications of chemical displacement to determine reaction kinetics have also been demonstrated and show that C−Br bond dissociation in vinyl bromide occurs near 157 K on Cu(110) and that toluene formation from the reaction of coadsorbed methyl iodide and phenyl groups occurs below 155 K on Cu(110).

Acknowledgment. Financial support from the National Science Foundation (Grants CHE-93-18625 and DMR-94-24296), from the Joint Services Electronics Program through

the Columbia Radiation Laboratory (Grant DAAG 55-97-1-0166), and from the Camille and Henry Dreyfus foundation in the form of a teacher−scholar award to B.E.B. is gratefully acknowledged.

References and Notes

(1) Bellot, J. C.; Condoret, J. S. *J. Chromatogr. A* **1993**, *657*, 305.
(2) Dijt, J. C.; Cohen Stuart, M. A.; Fleer, G. J. *Macromolecules* **1994**, *27*, 3219.
(3) Dijt, J. C.; Cohen Stuart, M. A.; Fleer, G. J. *Macromolecules* **1994**, *27*, 3229.
(4) Douglas, J. F.; Johnson, H. E.; Granick, S. *Science* **1993**, *262*, 2010.
(5) Kawaguchi, M.; Itoh, K.; Yamagiwa, S.; Takahashi, A. *Macromolecules* **1989**, *22*, 2204.
(6) Kawaguchi, M. *Adv. Colloid Interface Sci.* **1990**, *32*, 1.
(7) (a) Bien-Vogelsang, U.; Findenegg, G. H. *Colloids Surf.* **1986**, *21*, 469. (b) Siirila, A. R.; Bohn, P. W. *Langmuir* **1991**, *7*, 2188.
(8) (a) Barteau, M. A.; Madix, R. J. *Surf. Sci.* **1982**, *120*, 262. (b) Jorgensen, S. W.; Madix, R. J. *Surf. Sci.* **1983**, *130*, L291.
(9) Dickinson, E. *J. Chem. Soc., Faraday Trans.* **1992**, *88*, 3561.
(10) Zhang, Z.; Lagally, M. *Phys. Rev. Lett.* **1994**, *72*, 693.
(11) Rosenfeld, G.; Servaty, R.; Teichet, C.; Poelsema, B.; Comsa, G. *Phys. Rev. Lett.* **1994**, *71*, 895.
(12) Vrijmoeth, J.; van der Vergt, H. A.; Meyer, J. A.; Vlieg, E.; Behm, R. J. *Phys. Rev. Lett.* **1994**, *72*, 3843.
(13) Wakahara, A.; Vong, K. K.; Hasegawa, T.; Fujihara, A.; Sasaki, A. *J. Cryst. Growth* **1995**, *151*, 52.
(14) Collman, J. P.; Hegedus, L. S.; Norton, J. R.; Finke, R. G. *Principles and Applications of Organotransition Metal Chemistry*; University Science Books: Mill Valley, CA, 1987; Chapter 4.
(15) Yates, J. T., Jr.; Goodman, D. W. *J. Chem. Phys.* **1980**, *73*, 5371.
(16) Yamada, T.; Onishi, T.; Tamaru, K. *Surf. Sci.* **1983**, *133*, 33.
(17) Liu, A. C.; Friend, C. M. *Surf. Sci.* **1989**, *216*, 33.
(18) Jakob, P.; Menzel, D. *Surf. Sci.* **1989**, *220*, 70.
(19) Menzel, D.; Jakob, P. *Surf. Sci.* **1988**, *201*, 503.
(20) Xi, M.; Yang, M. X.; Jo, S. K.; Bent, B. E.; Stevens, P. *J. Chem. Phys.* **1994**, *101*, 9122.
(21) Ibbotson, D. E.; Wittrig, T. S.; Weinberg, W. H. *Surf. Sci.* **1980**, *97*, 297.
(22) Tsai, M.-C.; Stein, J.; Friend, C. M.; Muetterties, E. L. *J. Am. Chem. Soc.* **1982**, *104*, 3533.
(23) Tsai, M.-C.; Friend, C. M.; Muetterties, E. L. *J. Am. Chem. Soc.* **1982**, *104*, 2539.
(24) Friend, C. M.; Muetterties, E. L. *J. Am. Chem. Soc.* **1981**, *103*, 773.
(25) Tsai, M.-C.; Muetterties, E. L. *J. Phys. Chem.* **1982**, *86*, 5067.
(26) Tsai, M.-C.; Muetterties, E. L. *J. Am. Chem. Soc.* **1982**, *104*, 2534.
(27) Mitchell, G. E.; Henderson, M. A.; White, J. M. *Surf. Sci.* **1987**, *191*, 425.
(28) Campbell, C. T.; Rodriquez, J. A.; Henn, F. C.; Campbell, J. M.; Dalton, P. J.; Seimandies, S. G. *J. Chem. Phys.* **1988**, *88*, 6585.
(29) Henn, F. C.; Dalton, P. J.; Campbell, C. T. *J. Phys. Chem.* **1989**, *93*, 836.
(30) Hamza, A. V.; Ferm, P. M.; Budde, F.; Ertl, G. *Surf. Sci.* **1988**, *199*, 13.
(31) Muller, H.; Dierks, B.; Hamza, F.; Zagatta, G.; Fecher, G. H.; Bowering, N.; Heinzmann, U. *Surf. Sci.* **1992**, *269/270*, 207.
(32) Muller, H.; Dierks, B.; Fecher, G. H.; Bowering, N.; Heinzmann, U. *J. Chem. Phys.* **1994**, *101*, 7154.
(33) Kawai, M.; Toshinobu, J. *J. Electron Spectrosc. Relat. Phenom.* **1993**, *64/65*, 207.
(34) Lu, G.; Darwell, J. E.; Crowell, J. E. *J. Phys. Chem.* **1990**, *94*, 8326.
(35) Akerlund, C.; Zoric, I.; Hall, J.; Kasemo, B. *Surf. Sci.* **1994**, *316*, L1099.
(36) Lee, J.; Rettner, C. T. *J. Chem. Phys.* **1994**, *101*, 10185.
(37) Tamm, P. W.; Schmidt, L. D. *J. Chem. Phys.* **1970**, *52*, 1150.
(38) Shen, S.; Zaera, F.; Fischer, D. A.; Gland, J. L. *J. Chem. Phys.* **1988**, *89*, 590.
(39) Gland, J. L.; Fischer, D. A.; Shen, S.; Zaera, F. *J. Am. Chem. Soc.* **1990**, *112*, 5695.
(40) Parker, D. H.; Fischer, D. A.; Colbert, J.; Koel, B. E.; Gland, J. L. *Surf. Sci. Lett.* **1990**, *236*, L372.
(41) Parker, D. H.; Fischer, D. A.; Colbert, J.; Koel, B. E.; Gland, J. L. *Surf. Sci.* **1991**, *258*, 75.
(42) Zhang, R.; Gellman, A. J. *Langmuir* **1993**, *9*, 449.
(43) Madix, R. J.; Roberts, J. T. *Surf. Sci.* **1992**, *273*, 121.
(44) Nassir, M. H.; Fruhberger, B.; Dwyer, D. J. *Surf. Sci.* **1994**, *312*, 115.
(45) Regnier, J.; Bocke, C.; Dupont-Pavlovsky, N. *Surf. Sci.* **1981**, *112*, L770.
(46) Razafitianamaharavo, A.; Convert, P.; Coulomb, J. P.; Croset, B.; Dupont-Pavlovsky, N. *J. Phys. (France)* **1990**, *199*, 1961.
(47) Abdelmoula, M.; Ceva, T.; Croset, B.; Dupont-Pavlosky, N. *Surf. Sci.* **1992**, *272*, 167.
(48) Rodriquez, J. A.; Campbell, C. T. *J. Catal.* **1989**, *115*, 500.
(49) Rodriquez, J. A.; Campbell, C. T. *J. Phys. Chem.* **1989**, *93*, 826.
(50) Domagala, M. E.; Campbell, C. T. *Langmuir* **1994**, *10*, 2636.
(51) Columbia, M. R.; Thiel, P. A. *Surf. Sci.* **1990**, *235*, 53.
(52) Xi, M.; Bent, B. E. *Surf. Sci.* **1992**, *278*, 19.
(53) Fischer, D. A.; Colbert, J.; Gland, J. L. *Rev. Sci. Instrum.* **1989**, *60*, 1596.
(54) Outka, D. A.; Stohr, J. *J. Chem. Phys.* **1988**, *86*, 3539.
(55) Teplyakov, A. V.; Bent, B. E. *J. Am. Chem. Soc.* **1995,** *117*, 10076.
(56) Yang, M. X.; Eng, J., Jr.; Kash, P. W.; Flynn, G. W.; Bent, B. E.; Holbrook, M. T.; Bare, S. R.; Gland, J. L.; Fischer, D. A. *J. Phys. Chem.* **1996**, *100*, 12431.
(57) Kash, P. W.; Sun, D.-H.; Xi, M.; Flynn, G. W.; Bent, B. E. *J. Phys. Chem.* **1996**, *100*, 16621.
(58) Xi, M.; Bent, B. E. *Langmuir* **1994**, *10*, 505.
(59) Lin, J.-L.; Bent, B. E. *J. Am. Chem. Soc.* **1993**, *115*, 2849.
(60) Lin, J.-L.; Bent, B. E. *J. Phys. Chem.* **1993**, *97*, 9713.
(61) McQuarrie, D. A. *Statistical Mechanics*; Harper & Row: New York, 1976.